COBEM 2023 27TH INTERNATIONAL CONGRESS OF MECHANICAL ENGENEERING

ABCM Brazilian Society of Mechanical Sciences and Engineering
27th ABCM International Congress of Mechanical Engineering
December 04-08, 2023, Florianópolis-SC, Brazil

COB-2023-0274
THE DEVELOPMENT OF A DIDACTIC PLATFORM FOR WIND TUNNEL EXPERIMENTS IN APPLIED AERODYNAMICS

Rafael de Rezende Dias
Odenir de Almeida
Experimental Aerodynamics Research Center (CPAERO) - Federal University of Uberlandia (UFU), Rod 050 Km 78
rafaelrezendedias@ufu.br
odenir.almeida@ufu.br

Abstract. *This work was devoted to design, build, and test a real physic platform for wind tunnel measurements with the main goal of either demonstrating phenomena or validate and verify mathematical theories in Applied Aerodynamics. To provide real-life examples that bring students, especially those in Aeronautical and Mechanical Engineering courses, closer to the phenomena seen in problems that are more related to the daily life of an engineer, this project developed a robust problem based learning (PBL) experimental aerodynamics didactic platform, with the design, construction, instrumentation, qualitative and quantitative analysis of a series of wind tunnel experiments with circular cylinder models (2D), streamlined and non- aerodynamic bodies, and 2D and 3D wing profiles. All the models were built by using additive manufacturing through 3D printing with ABS and PLA. The models have been carefully finished with surface painting and later instrumented by inserting pressure taps, mounting rods and attachment points for aerodynamic balance. A robust series of data was collected and statistically treated in terms of lift and drag coefficients as well as pressure distribution and flow visualization. All gathered data in the wind tunnel tests were compared with theoretical results and similar experimental data available in literature providing very good agreement.*

Keywords: *Wind Tunnel, 3D printed, Airfoil, Experimental aerodynamics*

1. INTRODUCTION

Since the dawn of human flight, experimental aerodynamics played a crucial role in the understanding of the phenomena behind the interaction of the air with solid bodies. Wind tunnels offer a controlled environment in which the experimentalist can either validate the theorical approach or unfold a new array of hypothesis - Barlow and Pope (2015). In this sense, experimental aerodynamics can play an important role for the education of undergraduate students on mechanical and aeronautical engineering by giving a sense of the data collecting process and demonstrating, using real world examples, the application of the theory presented in class – Mason (2012). It is, therefore, crucial for the students enrolled in an experimental aerodynamics course to have access to a well-planned experimental setup, in order build a solid and incremental knowledge, avoiding unnecessary problems along the way.

This paper presents the process and results of the development of such a setup. Based on existing small scale commercial kits and on the available equipment at Federal University of Uberlandia – Brazil, a series of test subjects was designed to fill the needs of the students and to provide a robust experimental program.

The platform is structured accordingly to the subject sequency of the Applied Aerodynamics course. The goal of each experiment is to demonstrate a key point in each chapter. Beginning by introducing the students to the operation, calibration and data gathering of a wind-tunnel, followed by pressure readings and subsequent pressure coefficient calculations of cylinders, drag force and coefficient of different body shapes and, finally, airfoil (2D) and wing (3D) lift, drag and pressure distribution. By the end of the experimental program, the student is expected to have a comprehensive understanding ion of how the physical phenomena relates to inviscid flow models and how viscosity affects the results.

2. PROBLEM DESCRIPTION'S

2.1 Wind-Tunnel Calibration

The first experiment consists of a wind-tunnel calibration exercise, where students will have their first contact with the wind-tunnel and are expected to learn the basic operational procedures to conduct aerodynamic experiments safely and efficiently. The goal of this experiment is to produce a wind-tunnel calibration curve, based on the input frequency, Pitot tube velocity indications and pressure-based calculations using Bernoulli's equation for incompressible flow. In these experiments students will also verify the validity of Bernoulli's principle by applying it in a real-world experiment and comparing the resultant speed to the Pitot tube's value. Similar approach is seen in literature through the following works: Boyle (1988), Erm and Jacquemin (2015) and as described in GTTC Wind Tunnel Calibration Methodology Working Group (2018).

2.2 Pressure Coefficient Distribution over a Circular Cylinder

The second experiment consists of obtaining the pressure coefficient distribution around an infinite cylinder (2D). The results can then be compared to the theoretical predictions made by inviscid theory – Anderson (2011). In this experiment, a cylinder of diameter 100 mm was instrumented with pressure taps, is placed from end to end of the test section to avoid three-dimensional effects. Ten pressure ports are located along the surface of the cylinder, beginning at 0° (leading edge) and ending at 180° (trailing edge) over one hemisphere. The pressure differential is obtained using a 10-column water-manometer. The resultant differential pressure for each pressure port can then be used to calculate the local pressure coefficient. The final pressure coefficient curve is then compared to the theoretical curve and the Reynolds numbers are in the range of 10^4 - 10^5. This experiment also serves as a tool to prepare the students for the final experiment of this study, on which the pressure distribution over an airfoil is obtained. A complete review about flow over cylinders at different Reynolds numbers is reported by Zdravkovich (1997a and b).

2.3 Drag of Bluff and Aerodynamic Bodies

The third experiment aims at introducing the student to the operation of an aerodynamic balance and at showing the difference in drag of different body shapes. In this experiment, three body shapes are used: A circular flat plate, a sphere and an aerodynamic body, all 3D-printed with the same cross section radius and reference area. The bodies are attached to the aerodynamic balance via steel supports, the drag of which is measured beforehand. The Reynolds numbers in this setup is also of order $10^4 – 10^5$. This experiment also serves as a tool to prepare the students for next experiment, on which the aerodynamic balance is used to obtain the lift and drag forces of an Airfoil. Similar studies and data from drag of different shapes is found in the works of Roskho (1954), Hu & Zhou (2009), Yagmur et al. (2015) among others.

2.4 Airfoil Lift and Drag Coefficients

The next experiment setup aims at obtaining the lift and drag curves for a NACA4424 airfoil. The airfoil spans from end to end on the test section to reduce 3D flow effects and is fixated at the aerodynamic balance on one end and is left floating on the other end. Splitter plates are used on both sides to reduce the effect of the boundary layers of the tunnel. The curves of lift and drag versus angle of attack (AOA) are obtained by rotating the main rod that fixes the model to the aerodynamic balance to the desired geometric angle of attack and measuring the resultant lift and drag values. At the end of the experiment, the forces are dimensionless, and the curves are plotted as a function of the Reynolds number which in this experiment is of order 10^5. The flow over 2D-airfoils encounters several engineering applications and are extensively reported in literature such as Ahmed et al. (2007), Mueller & Batill (1982), Lee & Han (2020) among many others.

2.5 Airfoil Pressure Coefficient Distribution

The final experiment of this didactic series consists of obtaining the pressure distribution over the same NACA4424 airfoil. For this setup, the airfoil is instrumented with 35 pressure ports distributed along its upper and lower surfaces. The pressure ports are connected to an array of pressure sensors, which provide direct pressure readings when connect to a digital pressure transducer. The resultant plot may then be used to calculate the theoretical value of lift at moderate AOA ($\alpha < 5°$), which can then be compared to the values obtained on the previous experiment using the aerodynamic balance. Also, the Reynolds number in this setup is of order 10^5. Experimental pressure coefficient distribution over airfoil can be found in literature as example of Somers (1997), Nakano et al. (2007), Anyoji et al. (2014) among several others.

3. LABORATORY EQUIPMENTS

3.1 TV-60 Wind-Tunnel

The Laboratory for Experimental Aerodynamics at Federal University of Uberlândia (LAEX) is equipped with two active wind tunnels and expects a third to enter operational status soon. The TV-60 Zephyr Wind-Tunnel used for this research is a medium-size wind tunnel with maximum operational velocity of 26 m/s at the test section. It is equipped with a 25-horsepower electric motor which moves a 24-blade fan. The fan is located upwind of the test section as a blower and flow circuit was prepared with a set of guide-vanes and screens to control and guide the flow at the test section with low turbulence level (0.5% at high speeds). The test section has a cross section of 600 mm × 600 mm. The TV-60 Wind-Tunnel is shown in Fig.1.

The wind tunnel is equipped with a 3-component (lift, drag and moment) aerodynamic balance AA-TVAB1®, which is connected to computer. Measurements are either software-processed or gathered directly in the aerodynamic digital display.

Figure 1. Wind-Tunnel Zephyr TV-60 at LAEX.

The velocity of test section flow is measured using a L-type TPL-06-300 Pitot tube connected to a Kimo® MP200 digital manometer. For multiple pressure readings the tunnel can be equipped with analog pressure sensors (U-type water manometer) with 10 ports as well as digital pressure transducers, connected to an AA-TVCR2 64® channels pressure-module. Measurements of ambient conditions are gathered through a set of sensors for temperature and relative humidity - JIAXI model HTC-2A and barometric pressure and altitude - SUNROAD model Alt. All these equipment's were used in the different setups in this study, as described in the following sections.

4. EXPERIMENTS AND DATA

4.1 Wind-Tunnel Calibration

To validate the procedures intended to be used by the students, a preliminary wind tunnel calibration was performed using the Pitot tube and pressure manometer MP200 as the reference instrument. Two curve fittings were then performed using Matlab® to post-process the current data. The procedure consists of varying the electrical motor inverter frequency and reading the resultant flow velocity in the test section True airspeed and differential pressure was indicated by the pressure manometer and should be recorded either digitally or manually.

This apparatus has a declared accuracy of ± 0.5 % of reading ± 0.2 m/s for velocity values in the intended velocity range and ± 0.2 % or reading ± 0.8 Pa for values of pressure under 100 Pa and ± 0.2 % or reading ± 1.5 Pa for values above 100 Pa. The resulting calibration shows a good linear relation between the input frequency and output test section airflow velocity ($R^2 = 0.998$) as expected, showing a good flow quality in the test section.

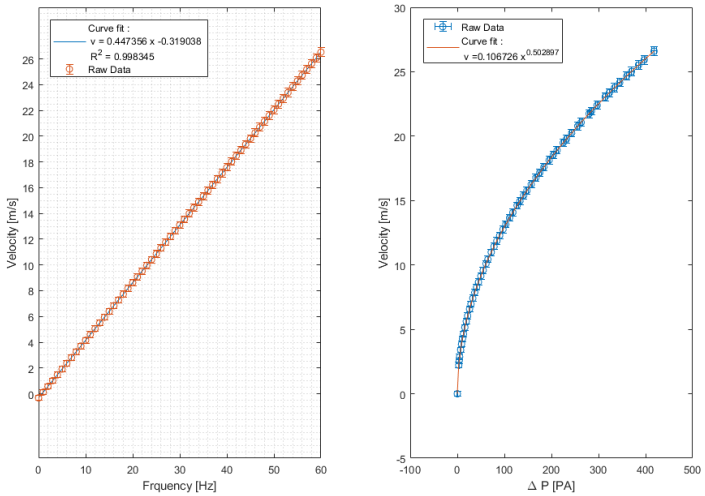

Figure 2. Wind-Tunnel TV-60 calibration results.

4.2 Pressure Coefficient Distribution over a Circular Cylinder

The distribution of C_p across a circular cylinder for an inviscid incompressible flow is described by Eq.1 from Anderson (2011).

$$C_p = 1 - 4sin^2(\theta) \tag{1}$$

where θ is the angular position across the surface of the cylinder, 0° being the leading edge and 180° being the trailing edge. The distribution is symmetrical for the upper and lower surfaces of the cylinder. For viscous flow, this symmetry is violated due to flow separation and viscous effects as also described in Anderson (2011).

For this experiment, 10 holes were drilled on the surface of a 100 mm diameter PVC tube adequately prepared for gathering this instrumentation. The 10 pressure ports were connected to the pressure transducer module via flexible silicone hoses with an internal diameter of 1.6 mm. The cylinder was then placed vertically from end to end of the test section, as depicted by Fig.3.

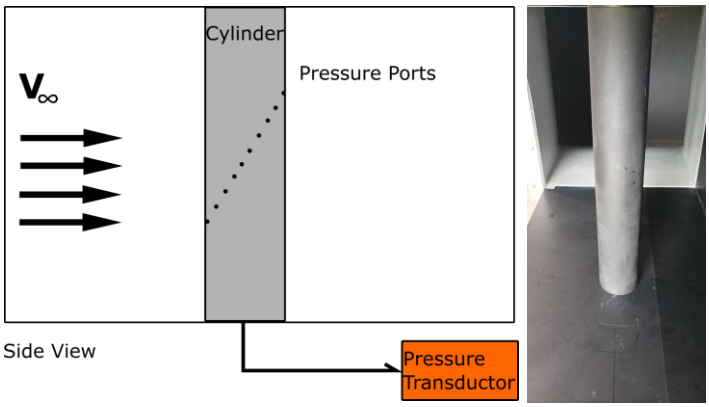

Figure 3. Cylinder experiment schematic and real model.

Table 1 shows the location of each pressure port, the channel to which its connected and the operational limits of each channel accordingly to the pressure module manufacturer's datasheet. The accuracy is described as 0.5 % of the operational limit of each channel. The measurements were taken in 5 different Reynolds numbers, for each Reynolds number the experiment was repeated 3 times, using an average of 650 datapoints for each run at an acquisition time rate of 0.2 s for sample. The results for the pressure distribution are shown in Figure 4.

Table 1. Angular position, channel, and operational limit of each pressure port on the surface of the cylinder.

Angular Position	Channel	Operational Limit
0°	1	02 kPa
20°	2	02 kPa
40°	3	02 kPa
60°	4	02 kPa
80°	5	02 kPa
100°	6	02 kPa
120°	7	02 kPa
140°	8	02 kPa
160°	33	10 kPa
180°	40	10 kPa

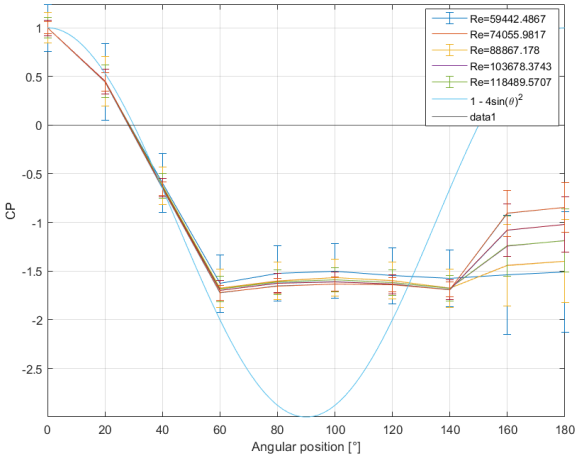

Figure 4. Pressure coefficient distribution over a circular cylinder - Experimental results.

The results are consistent with the inviscid incompressible flow theory for angular positions as high as 60°, at which point viscous effects become dominant and the experimental pressure stabilizes for all Reynolds numbers. For positions as high as 160°, the boundary layer separation can be perceived as the experimental data fails to follow the pressure buildup predicted by inviscid flow theory – Anderson (2011).

4.3 Drag of Bluff and Aerodynamic Bodies

Three different bodies were used in this experiment to reproduce classical shapes and data from literature. To maintain the same wind tunnel blockage as recommended by Barlow & Pope (1999), all models have a maximum frontal area radius of 100 mm. The models were then drawn using Solidworks® and later 3D-printed by using a Makerbot Replicator Z18 machine. To have a good surface rugosity, a thin layer of surface finishing was added, and the final models were then polished. The steel support rod had to be custom-made to guarantee the centralized position of the models on the test section. For this experiment, the aerodynamic balance AA-TVAB1® was used to obtain the drag force values with the maximum lift of order 400 N while maximum drag is 50 N with an accuracy of 0.8 % and resolution of 0.01 N. To account for the setup interference on the experiment, the drag force of each support was previously measured and subtracted from the total drag measured for each support-body couple. Next, the description of each body is provided:

4.3.1 Flat Plate

The first body consists of a flat plate placed perpendicularly to the flow. The flat plate was fixated to the aerodynamic balance via an aluminum rod with a threaded 90º bend on its end, forming an elbow support, as can be seen on Figure 5.

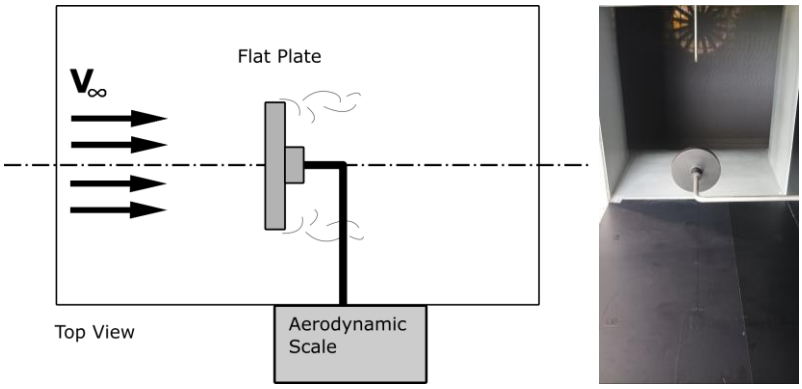

Figure 5. Flat plate model – schematic and real model.

4.3.2 Sphere

The sphere uses the same support as the flat plate as depicted by Figure 6.

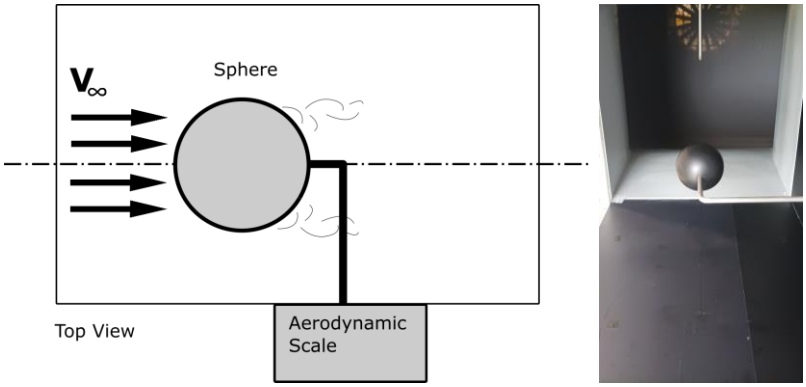

Figure 6. Sphere model – schematic and real model.

4.3.3 Aerodynamic Body

For the aerodynamic body, a flat steel rod was designed as to keep longitudinal axis of the aerodynamic body centered with the centerline of the test section of the tunnel. The complete setup is illustrated in Figure 7.

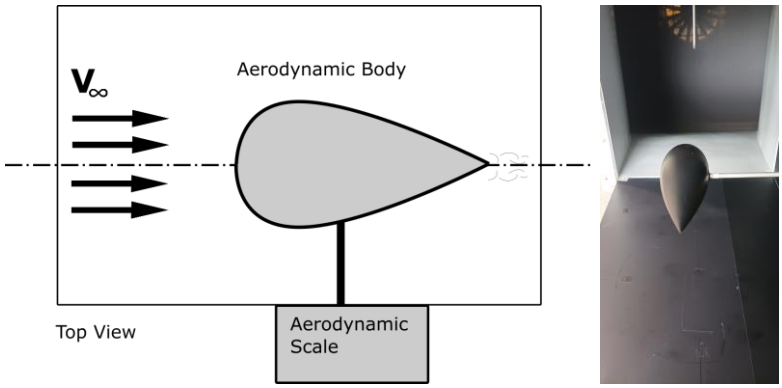

Figure 7. Aerodynamic body – schematic and real model.

4.3.4 Drag Results for Bluff and Aerodynamic Bodies

The expected drag coefficient values, based on literature review, for the sphere range from 0.47 to a smooth sphere and 1.17 to a smooth flat plate for Reynolds numbers ranging from 10^4 to 10^6 – Hoerner (1965).

To enable a better comparison, all three bodies were designed as to have the same frontal area of $7.9x10^{-3}\ m^2$, as previously discussed. Figure 8 provides the results of the total drag force and drag coefficient of each body as a function of Reynolds Number.

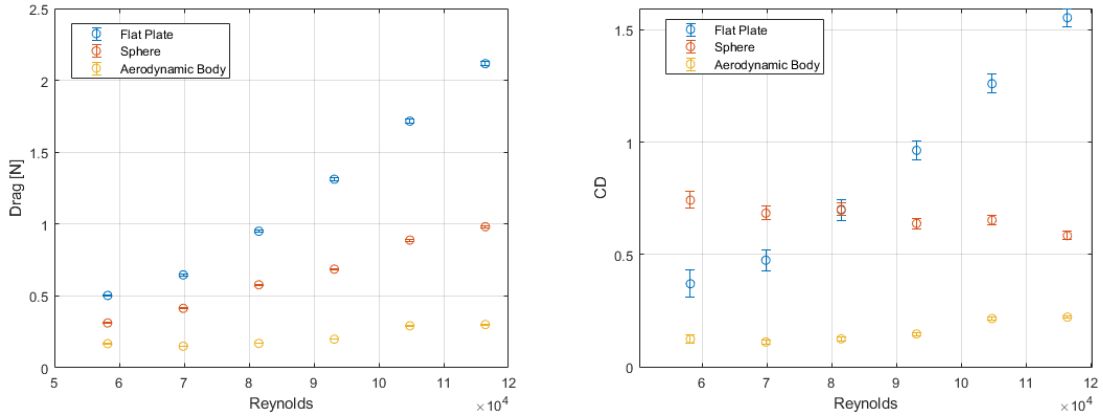

Figure 8. Aerodynamic drag force and coefficient as a function of Reynolds Number.

The results present a consistent behavior of Drag force values and drag coefficient as the Reynolds number grows and could be compared with data from literature, as described by Hoerner (1965).

4.4 Airfoil

For the airfoil experiments covering lift, drag and pressure distribution measurements, a NACA 4424 airfoil was chosen for its significant thickness, which enables easy access to the interior for the assembly, facilitating the installation of pressure ports and hoses. The next subsections describe the airfoil apparatus used for both experimentations.

4.4.1 Airfoil Lift and Drag

To obtain the lift and drag curves, a 3D-printed and surface finished NACA4424 airfoil was fixed on both ends of the test section. On each extremity, a splitter-plate was used to minimize the wall interference. Figure 9 shows the setup schematic and real model assembled in the wind tunnel test section.

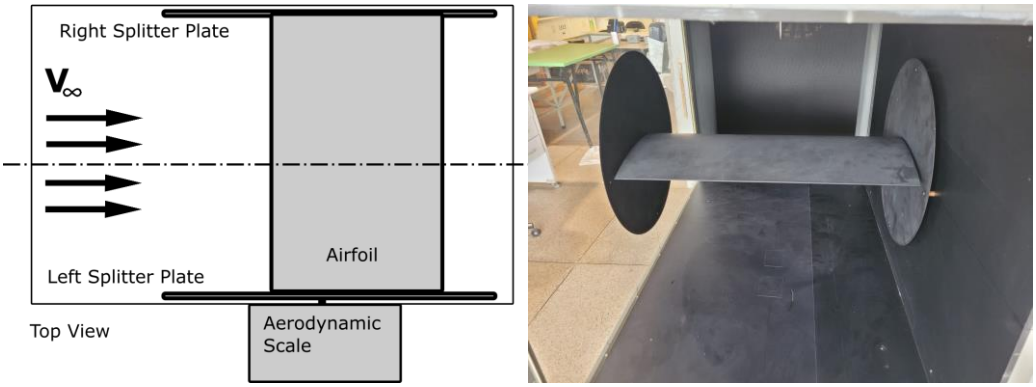

Figure 9. Airfoil Lift and Drag experiment schematic.

The airfoil dimensions are respectively, chord = 250 mm, span = 565.2 mm and planform area of 141300 mm^2. The test was performing varying the geometric angle of attack of the airfoil in 1° per run. For each test run, 10 measurements of lift and drag were taken. The experiment was performed for a Reynolds number of $2\,x\,10^5$. Figure 10 shows the resulting lift and drag coefficient curves as a function of angle of attack, as well as the data obtained from XFOIL for comparison purposes – Drela (1989).

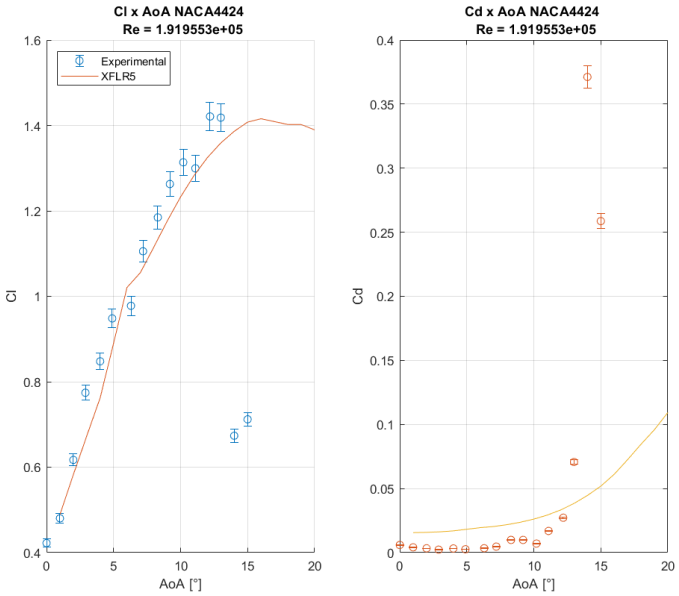

Figure 10. Airfoil lift and drag coefficient curves.

The experimental results show good consistency with low-speed airfoil theory and XFOIL data for low angles of attack, presenting a consistent $C_l \times \alpha$ curve. However, at higher AOA some discrepancy is seen against XFOIL data. This is expected to happen due to the Re number of the experiment where viscous effects play important role on the flow pattern. The airfoil stalls at around 14°, at which point a peak in drag occurs – Anderson (2011).

4.4.2 Airfoil Pressure Distribution

For the pressure distribution experiment, the NACA 4424 was equipped with 35 pressure ports connected to the AA-TVCR2 64® pressure module. Figure 11 shows the experiment schematic and real assembly in the wind tunnel.

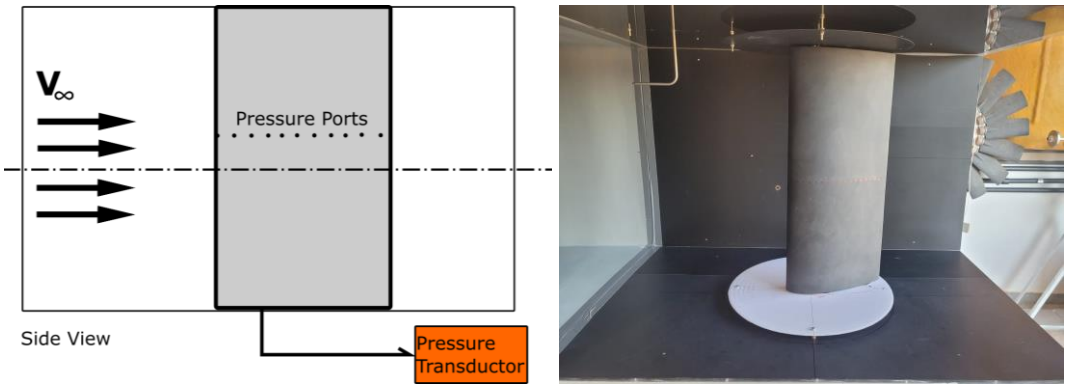

Figure 11. Airfoil pressure experiment – schematic and real model.

The airfoil was manufactured using 3D-print capabilities, as previously discussed, by using the same CAD model used to the aerodynamic balance experiment, with the only addition being 35 pressure ports at the central section of the model. Splitter plates were used on both sides of the test section to minimize the interference of the tunnel wall boundary layer and approximate the results to those of infinite wing theory. The only difference is that this model was assembled in the vertical position in the test section to facilitate the pressure cabling and connection to the pressure transducer module, that was placed underneath.

For cable management reasons, the spatial distribution of pressure ports and its respective pressure channels were organized in the following way: pressure ports of numbers 1 up to 18 were placed in the upper surface of the airfoil with operational limit varying from 2 kPa up to 50 kPa due to resolution of the available channels in the pressure transducer; pressure ports of numbers 19 up to 35 were placed in the lower surface with operational limit varying from 10 kPa up to 50 kPa.

The experiment was conducted on a Reynolds number of $2\ x\ 10^5$ to better match the data with the aerodynamic scale experiment. The angle of attack was varied from 0° to 14°, in which is the airfoil was in pre stall condition. Figures 12 and 12 depicts the resultant pressure coefficient curves for each angle of attack, as well as the correspondent XFOIL results, for comparison purposes.

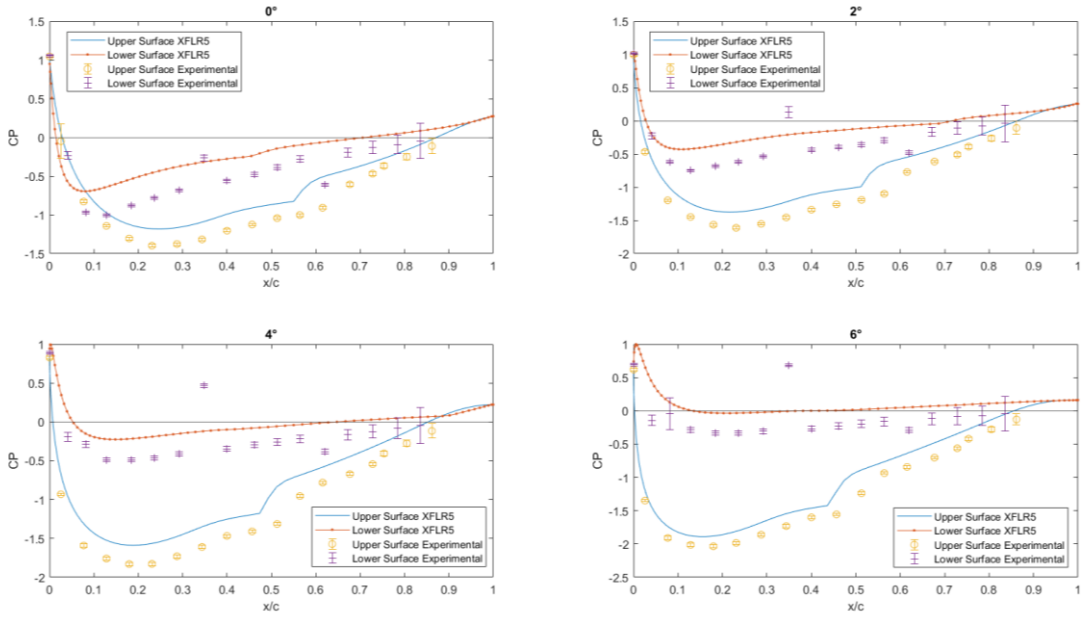

Figure 12. Pressure coefficient results for AOA (α) 0° up to 6°.

The results were consistent showing good pattern in the Cp × α curves. The pressure port 26, located in the lower surface of the airfoil presented wrong data with high standard deviation. Later, it was concluded that this port had problem's connection with the pressure transducer. The data was kept in the plots to show this discrepancy as part of the students 'experimental learning procedure.

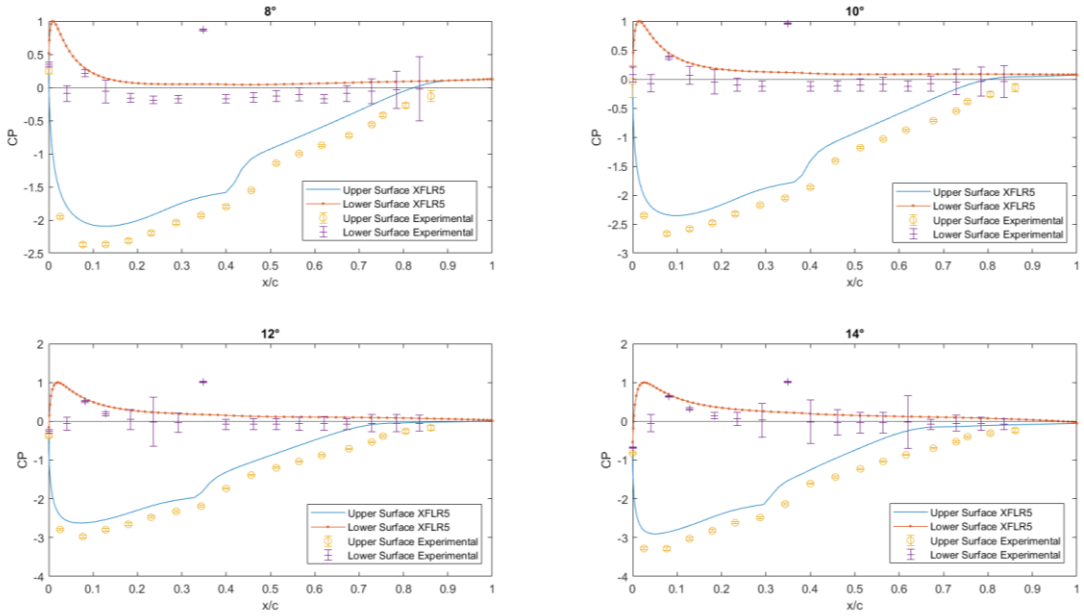

Figure 13. Pressure coefficient results for AOA (α) 8° up to 14°.

5. CONCLUSION

This work aimed to build a robust and didactic sequence of experiments for use in undergraduate experimental aerodynamics courses associated with Mechanical and Aeronautical engineering formation. In this context, at set of experimental apparatus was built and assembled in the low-speed wind tunnel equipped with proper instrumentation to achieve reasonable and satisfactory database on different problems. By carrying out this set of experiments, it is expected that students involved in the learning process will be able to have contact with measurement techniques in a wind tunnel,

namely measuring velocity profiles, aerodynamic forces (drag and lift) as well as pressure distribution over bodies. Additionally, students are expected to have knowledge about the limitations of some aerodynamic theories and to experimentally evaluate the real effects present in such canonical problems, such as viscous effects and boundary layer separation. The good agreement between the results collected and those predicted by theory and numerical methods attests to the success of this undertaking.

Throughout experiment assembly phase, some difficulties concerning the test section setup arose, specifically regarding the extensive period needed to set an experiment, which may be especially problematic if time between experiments is short, a common situation in engineering courses. Improvements in this field are being planned by the LAEX team. Proper documentation of the experiment assembly sequency is also in progress may also be developed, to further reduce the time needed between experiments. Instrument calibration is critical to ensure correct data acquisition. In this regard, considering the high demand for wind tunnel use at UFU, it is recommended that this calibration is performed at least at the start of each school year for the teaching experiments and for each research project just prior the start of the specific experiment. Finally, this article serves as a reference for other similar studies and as a guide and aid for Brazilian universities that wish to set up an experimental apparatus for teaching experimental aerodynamics.

6. REFERENCES

Barlow, J. B., Rae Jr, W. H., & Pope, A. (2015). Low speed wind tunnel testing. INCAS Bulletin, 7(1), 133.

MASON, W. (1992, January). What we need in experimental aerodynamics-One engineering educator's view. In 30th Aerospace Sciences Meeting and Exhibit (p. 161).

Boyle, M. T. (1988, February). Low speed wind tunnel testing. In Fourth annual IEEE semiconductor thermal and temperature measurement symposium (pp. 31–39). San Diego, CA, USA. IEEE.

Erm, L. P., Jacquemin, P. P., & DEFENCE SCIENCE AND TECHNOLOGY ORGANISATION FISHERMANS BEND (AUSTRALIA) FISHERMANS BEND Australia. (2015). Calibration of the flow in the test section of the research wind tunnel at DST Group (p. 0031). Technical Note 1468, Aerospace Division, Defence Science and Technology Group.

GTTC Wind Tunnel Calibration Methodology Working Group. (2003). Recommended Practice: Calibration of Subsonic and Transonic Wind Tunnels (AIAA R-093-2003 (2018)).

Anderson, J. D. (2011). Fundamentals of Aerodynamics. McGraw Hill Education.

Jewel B. Barlow, W. H. (1999). Low-Speed Wind Tunnel Testing. Wiley-Interscience.

Zdravkovich, M. M. (1997). Flow around circular cylinders: Volume 1: Fundamentals (Vol. 1). Oxford university press.

Zdravkovich, M. M. (1997). Flow around circular cylinders: Volume 2: Applications (Vol. 2). Oxford university press.

Roshko, A. (1954). On the drag and shedding frequency of two-dimensional bluff bodies (No. NACA-TN-3169).

Hu, J. C., & Zhou, Y. (2009). Aerodynamic characteristics of asymmetric bluff bodies.

Yagmur, S., Dogan, S., Aksoy, M. H., Canli, E., & Ozgoren, M. (2015). Experimental and numerical investigation of flow structures around cylindrical bluff bodies. In EPJ Web of Conferences (Vol. 92, p. 02113). EDP Sciences.

Ahmed, M. R., Takasaki, T., & Kohama, Y. (2007). Aerodynamics of a NACA4412 airfoil in ground effect. AIAA journal, 45(1), 37-47.

Mueller, T. J., & Batill, S. M. (1982). Experimental studies of separation on a two-dimensional airfoil at low Reynolds numbers. AIAA journal, 20(4), 457-463.

Lee, S. H., & Han, Y. O. (2020). Experimental investigation of high-angle-of-attack aerodynamics of low-aspect-ratio rectangular wings configured with NACA0012 airfoil section. International Journal of Aeronautical and Space Sciences, 21, 303-314.

Somers, D. M. (1997). Design and experimental results for the S809 airfoil (No. NREL/SR-440-6918). National Renewable Energy Lab.(NREL), Golden, CO (United States).

Nakano, T., Fujisawa, N., Oguma, Y., Takagi, Y., & Lee, S. (2007). Experimental study on flow and noise characteristics of NACA0018 airfoil. Journal of Wind Engineering and Industrial Aerodynamics, 95(7), 511-531.

Anyoji, M., Nonomura, T., Aono, H., Oyama, A., Fujii, K., Nagai, H., & Asai, K. (2014). Computational and experimental analysis of a high-performance airfoil under low-Reynolds-number flow condition. Journal of Aircraft, 51(6), 1864-1872.

Barlow, J. B., Rae, W. H., & Pope, A. (1999). Low-speed wind tunnel testing. John wiley & sons.

Hoerner, S. F. (1965). Fluid-Dynamic Drag. Theoretical, experimental and statistical information. Copyright by: SF Hoerner Fluid Dynamics, Vancouver, Printed in the USA, Card Number 64-19666.

Drela, M. (1989, June). XFOIL: An analysis and design system for low Reynolds number airfoils. In Low Reynolds Number Aerodynamics: Proceedings of the Conference Notre Dame, Indiana, USA, 5–7 June 1989 (pp. 1-12). Berlin, Heidelberg: Springer Berlin Heidelberg.

7. RESPONSIBILITY NOTICE

The author(s) is (are) the only responsible for the printed material included in this paper.